# A deep variational free energy approach to dense hydrogen

Hao Xie, 1,2 Zi-Hang Li, 1,2 Han Wang, 3,\* Linfeng Zhang, 4,5,† and Lei Wang 1,6,‡

1 Beijing National Laboratory for Condensed Matter Physics and Institute of Physics,
Chinese Academy of Sciences, Beijing 100190, China

2 School of Physical Sciences, University of Chinese Academy of Sciences, Beijing 100190, China

3 Laboratory of Computational Physics, Institute of Applied Physics and Computational Mathematics,
Huayuan Road 6, Beijing 100088, China

4 DP Technology, Beijing 100080, China

5 AI for Science Institute, Beijing 100080, China

6 Songshan Lake Materials Laboratory, Dongguan, Guangdong 523808, China
(Dated: September 14, 2022)

We present a deep generative model-based variational free energy approach to the equations of state of dense hydrogen. We employ a normalizing flow network to model the proton Boltzmann distribution and a fermionic neural network to model the electron wavefunction at given proton positions. By jointly optimizing the two neural networks we reached a comparable variational free energy to the previous coupled electron-ion Monte Carlo calculation. Our result suggests that hydrogen in the planetary condition is even denser compared to previous Monte Carlo and *ab initio* molecular dynamics data, which is further away from the empirical chemical model predictions. Obtaining reliable equations of state of dense hydrogen, and in particular, direct access to entropy and free energy opens new opportunities in planetary modeling and high-pressure physics research.

Hydrogen is the most abundant element in the visible universe. It is also the first and the simplest element in the periodic table, consisting of only a proton and an electron. Despite its simplicity, high-pressure dense hydrogen exhibits rich physical phenomena [1] such as metallization [2] and high-temperature superconductivity [3]. A thorough understanding of these phenomena is of fundamental importance to a broad range of disciplines including planetary physics [4] and nuclear fusion [5]. For these reasons, accurate prediction of the equations of state and phase diagram of dense hydrogen has been a touchstone for computational methods.

Dense hydrogen is a quantum many-body system consisting of coupled protons and electrons. Due to large difference in the mass of electron and proton, it is often reasonable to employ the Born-Oppenheimer approximation [1], in which protons move in an effective potential obtained by solving the electronic Hamiltonian with fixed proton positions. Since the energy scale of electrons is much higher than that of protons, even a tiny error in the electronic calculation could yield a significant error in the predicted proton configurations. Standard ab initio molecular dynamics (MD) [6] solves the electronic structure problem using density functional theory calculations, whose reliability depends on the specific choice of density functionals [7]. Using machine-learned potential energy surfaces can push such MD simulations to much larger system sizes and longer times [8, 9]. However, such an approach at most reflects the accuracy of the underlying electronic structure model that generates the training data, and the reliability issue still persists [10–14].

A more reliable method to solve the many-electron system is the quantum Monte Carlo method [15]. In the context of dense hydrogen, one can sample the proton con-

figurations according to stochastic estimates of the energy or force acting on the protons, as were previously done in the coupled electron-ion Monte Carlo (CEIMC) [16] method and Langevin MD [17], respectively. However, these nested Monte Carlo approaches have two unsatisfactory drawbacks. Firstly, the statistical noises in the estimated energy or force hamper an unbiased sampling of the protons, similar to the case of Bayesian inference with noisy log-likelihood functions [18]. There have been three remedies in the literature: a) the noisy Monte Carlo approach [19] assumes the noises are sufficiently small and treats the acceptance rate using the von Neumann-Ulam method; b) the penalty method [20] assumes that the noisy energy estimates follow the Gaussian distribution and reduces the acceptance rate with an empirically estimated variance; c) the stochastic gradient Langevin dynamics [17, 21, 22] relies on sufficiently small integration steps with noisy forces to sample from the correct Boltzmann distribution. In all cases, statistical uncertainties in the energy functions deteriorate the sampling efficiency and may even introduce bias to the results. These downsides have partially reduced the reliability advantage of employing the more sophisticated quantum Monte Carlo solver for dense hydrogen. For example, suppose one has obtained different results with different flavors of quantum Monte Carlo methods or initial proton configurations, it is rather difficult to tell which results to trust. Secondly, the nested nature of the approach makes the computation very demanding: one has to make the inner electronic calculation fully converge to ensure correct sampling of the Born-Oppenheimer potential energy surface of protons. Such a stringent requirement makes it rather tedious to ensure convergence of the method [23, 24] or limits one to manuallycrafted variational wavefunctions with a few or even no variational parameters [25, 26].

In light of these difficulties faced by the nested Monte Carlo approaches [16, 17], we introduce a deep generative model-based variational free energy approach for the dense hydrogen problem. We will minimize the variational free energy with

<sup>\*</sup> wang\_han@iapcm.ac.cn

<sup>†</sup> linfeng.zhang.zlf@gmail.com

<sup>\*</sup> wanglei@iphy.ac.cn

respect to a trial density matrix [27]

$$F = k_B T \text{Tr}(\rho \ln \rho) + \text{Tr}(\rho H), \tag{1}$$

with the two terms being entropy and energy respectively;  $k_B$ is the Boltzmann constant and T is the temperature. Although free energy minimization is a fundamental principle in quantum statistical mechanics, its practical application is inhibited by the intractable computational cost of entropy term [28]. Recent advances in deep generative models [29] have removed this road blocker. Variational free energy calculations based on deep generative models have been applied to a wide range of problems including the Ising models [30-32], lattice field theories [33, 34], atomic solids [35, 36], quantum dots [37], and uniform electron gases [38]. In particular, due to the difficulties of alternative approaches, the deep generative model-based variational free energy methods have the potential to become an indispensable tool for many-fermion problems at finite temperature, such as Refs. [37, 38] and the hydrogen problem considered here.

We represent the density matrix  $\rho$  using two neural networks as shown in Fig. 1, one for the proton Boltzmann distribution and one for the electron wavefunction. Variational free energy calculation of Eq. (1) then amounts to solving a stochastic optimization problem [39]. In such a formulation, the statistical noises in the estimated energy will not be as catastrophic as in the Monte Carlo sampling [16, 17]. In this way, the present approach trades the shortcomings of nested Monte Carlo approaches [16, 17] with a variational bias. However, by making use of deep neural network ansatz one can largely overcome this issue by continuously lowering the variational free energy. With further systematic improvements of variational ansatz and optimization schemes, we anticipate one will reach a reliable description for the whole phase diagram of dense hydrogen with the variational free energy approach.

Consider N protons and N electrons in a periodic cubic box of volume  $L^3$ . The system is unpolarized so there are N/2 spin-up and spin-down electrons respectively. The density of the system is specified by the dimensionless parameter  $r_s = \left(\frac{3}{4\pi N}\right)^{1/3} L/a_0$ , where  $a_0$  is the Bohr radius. In the atomic units, the Hamiltonian of the hydrogen system reads

$$H = \sum_{i} \frac{-\nabla_{i}^{2}}{2} + \sum_{i < j} \frac{1}{|\mathbf{r}_{i} - \mathbf{r}_{j}|} + \sum_{I < J} \frac{1}{|\mathbf{s}_{I} - \mathbf{s}_{J}|} - \sum_{i, I} \frac{1}{|\mathbf{r}_{i} - \mathbf{s}_{I}|}, (2)$$

where  $S = \{s_I\}$  and  $R = \{r_i\}$  denote the proton and electron coordinates, respectively. Note the Fermi temperatures of proton and electron are well separated due to their large mass difference. For a wide temperature range that falls in between these two temperature scales, one can treat protons as classical particles and assume the electrons stay in their instantaneous ground state under given proton configuration. For this reason, we have neglected the proton kinetic energy term in Eq. (2).

The variational density matrix of dense hydrogen under consideration is diagonal with respect to the proton degrees of freedom, and can be written as  $\rho = \int dS p(S) |S, \psi_S\rangle \langle S, \psi_S|$ .

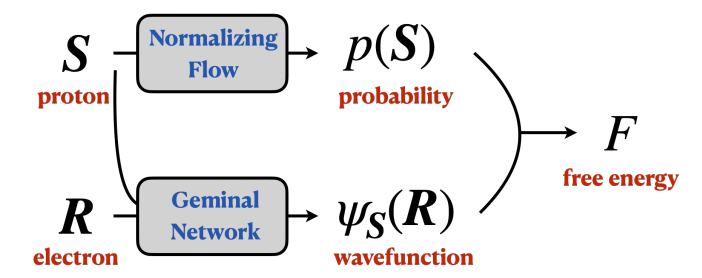


FIG. 1. A sketch of computational graph for the dense hydrogen problem. The model consists of a normalizing flow Eq. (3) for the proton Boltzmann distribution and a geminal neural network Eq. (4) for the electron wavefunction with fixed proton positions. We jointly optimize the two neural networks to minimize the variational free energy Eq. (1).

p(S) is a normalized probability density for the proton coordinates, and  $|S, \psi_S\rangle \equiv |S\rangle \otimes |\psi_S\rangle$  is a basis of the whole system's Hilbert space, where  $|\psi_S\rangle$  is the electronic ground state at fixed proton configuration S. The variational free energy  $F = \int dS \ p(S) \left[ k_B T \ln p(S) + \langle \psi_S | H | \psi_S \rangle \right]$  consists of the entropy of the proton Boltzmann distribution and the electronic expected energy weighted over the proton configurations [40].

We parametrize the proton Boltzmann distribution p(S) using a normalizing flow network. Normalizing flow is a class of deep generative model that represents high-dimensional probability density using change-of-variables transformations [41]. Specifically, assuming  $\zeta$  is a set of independent and uniformly distributed "collective" coordinates, we use a neural network to implement a learnable bijective mapping between  $\zeta$  and the original proton coordinates S. The resulting probability density for protons then reads

$$p(S) = \frac{1}{L^{3N}} \left| \det \left( \frac{\partial \zeta}{\partial S} \right) \right|. \tag{3}$$

Note this expression is normalized, which facilitates a straightforward and easy computation of the entropy term in the variational free energy objective Eq. (1). We construct the bijective transformation between  $\zeta$  and S as a residual network using the fermionic neural network layers [42]. Since each layer is permutation equivariant, Eq. (3) is invariant to the permutation of proton coordinates [43]. Moreover, the construction also ensures translational invariance and periodicity of the probability density [40]. We compute the transformation Jacobian in Eq. (3) using forward-mode automatic differentiation [44].

Next, we design a neural network for the electronic ground-state trial wavefunction  $\psi_S(R) \propto \langle R | \psi_S \rangle$  at fixed proton positions. We concatenate the proton and electron coordinates together and feed them into a fermionic layer [42] which accounts for the periodic boundary conditions and translational invariance [38, 45–48]. The layer outputs  $f^S \in \mathbb{R}^{N \times M}$  and  $f^\uparrow, f^\downarrow \in \mathbb{R}^{N/2 \times M}$ , which are features that transform equivariantly under the permutation of protons and electrons of the same spin. Using these features, we construct an unnormalized Jastrow-geminal-type wavefunction [40]

$$\psi_{S}(\mathbf{R}) = e^{J} \det (G \circ D), \tag{4}$$

where  $J = \sum_{i,\mu} a_{\mu} f_{i\mu}^{S}$  serves as a Jastrow factor, and  $\circ$  denotes an element-wise product between two matrices.  $G_{ij} =$  $\sum_{\mu,\nu} \chi_{i\mu}^{\uparrow} W_{\mu\nu} \chi_{j\nu}^{\downarrow}$  is a  $N/2 \times N/2$  geminal matrix that depends on a real-valued parameter matrix W. Here,  $\chi^{\uparrow}$  and  $\chi^{\downarrow} \in \mathbb{C}^{N/2 \times M}$ are complex orbital functions obtained from a linear map of the  $f^{\uparrow}$  and  $f^{\downarrow}$  features respectively. On the other hand,  $D_{ij} = \sum_k \lambda_k e^{ik\cdot(z_i^\uparrow - z_j^\downarrow)}$  is an envelope function formed by several plane-wave states with backflow coordinates  $z^\uparrow$  and  $z^\downarrow$ .  $\lambda_k$ are learnable positive parameters representing the occupation number for the momenta  $k = \frac{2\pi n}{L}$  ( $n \in \mathbb{Z}^3$ ). We use a large number of k-points in the summation so that the wavefunction can easily capture oscillatory features. The feature size M can be regarded as the number of orbitals. When M > N/2, a single geminal determinant would correspond to a summation of combinatorially large  $\binom{M}{N/2}$  number of determinants according to the Cauchy-Binet formula. The fermionic neural network [42] construction of the orbitals  $\chi^{\uparrow}$  and  $\chi^{\downarrow}$  further boosts the expressibility of the ansatz compared to the well-known geminal states with Jastrow factors [49]. One can verify that besides being antisymmetric under permutation of electrons of the same spin to account for their fermionic nature, the wavefunction Eq. (4) is also permutation invariant with respect to the proton coordinates. Note the present architecture design is more lightweight than that of [50, 51] regarding the goal of respecting permutation symmetry of the same type of nuclei.

By parametrizing the hydrogen density matrix using two neural networks, the variational free energy calculation of Eq. (1) reduces to the following stochastic optimization problem

$$\min_{\phi,\theta} \mathbb{E}_{S \sim p(S)} \left[ k_B T \ln p(S) + \mathbb{E}_{R \sim |\psi_S(R)|^2} \left[ \frac{H\psi_S(R)}{\psi_S(R)} \right] \right], \quad (5)$$

where  $\phi$ ,  $\theta$  are variational parameters of the proton Boltzmann distribution Eq. (3) and the electronic ground-state wavefunction Eq. (4), respectively. We employ the Markov-Chain Monte Carlo algorithm to draw proton and electron coordinate samples from the two models in an ancestral manner. As for optimization, we have used a generalized stochastic reconfiguration method [49] for density matrices, which is very similar to a recent variational free energy calculation of finite-temperature electron gases [38]. Note, however, that some subtle yet important modifications have to be made, which originate from the fact that the electron wavefunction ansatz Eq. (4) adopted in this work is unnormalized [40]. Since the proton Boltzmann distribution and electron wavefunction are optimized in a joint way, one does not need to wait for an expensive inner optimization loop to fully converge before moving the protons. At a conceptual level, jointly moving the nuclear and electronic degrees of freedom is akin to the Car-Parrinello molecular dynamics [6], yet in a more coherent variational optimization framework.

We employ twist-averaged boundary conditions (TABC) [52] in the calculation to reduce the finite-size effects, in particular those originating from the single-particle momentum shell structure. This amounts to adding a twist angle to the momenta  $k \to k + q$  in Eq. (4), with  $q \in [-\frac{\pi}{l}, \frac{\pi}{l}]^3$ .

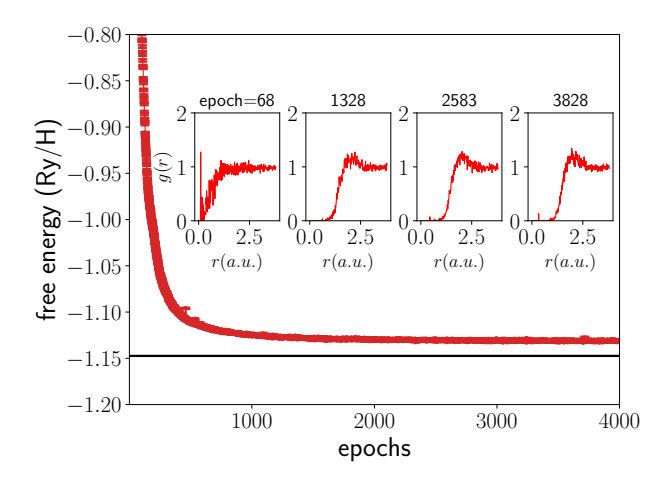


FIG. 2. Variational free energy per atom versus optimization epochs of N=54 hydrogen atoms at T=6000K and  $r_s=1.25$ . The horizontal line shows the free energy obtained by coupling-constant integration of CEIMC energies [53]. The inset shows the proton-proton pair correlation functions at several different training epochs.

In practice, we sample q from a uniform distribution along with the proton coordinates, which does not increase the simulation efforts. To improve the accuracy of electronic ground-state calculation, we have also introduced explicit twist dependence in the wavefunction ansatz [40].

As a first application of the deep variational free energy approach, we focus on dense hydrogen at planetary conditions, where it is an ionized liquid of protons and electrons. Equations of state of dense hydrogen under such a condition are crucial for the model of giant planets' interiors [4]. For these applications, it is crucial to compute the entropy so that one can follow the adiabatic curve from the planet's surface to its interior [54]. However, standard Monte Carlo methods do not have direct access to the entropy. Ref. [53] employed the coupling-constant integration method based on CEIMC calculations to obtain the free energy and entropy of dense hydrogen at T = 6000K and  $r_s = 1.25$ . This result was then used as the anchor point to obtain the full equation of state of dense atomic hydrogen.

We carry out deep variational free energy calculation at the same parameters T = 6000K and  $r_s = 1.25$  as [53]. We initialize the neural network parameters in Eqs. (3) and (4) such that the proton density starts from a uniform distribution and the electron wavefunction starts from a plane-wave state. Figure 2 shows the decrease of the variational free energy with training epochs. The variational free energy reaches a slightly higher value compared to Ref. [53]. Moreover, we observe that the entropy of the proton distribution also decreases with training due to the protons learning to develop a more informative distribution starting from the initial uniform distribution. The insets of Fig. 2 show the proton-proton pair correlation functions develop a structure as the training proceeds. Note that despite the free energy varies only a little in the later stage of training process, the correlation functions still undergo quite significant changes.

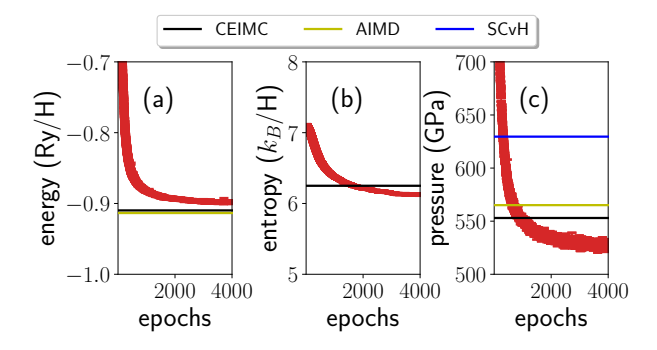


FIG. 3. (a) Internal energy, (b) entropy per hydrogen atom, and (c) pressure versus the training epochs. The system parameters are the same as Fig. 2. The horizontal black line shows the CEIMC results of [53]. The yellow and blue lines show the *ab initio* MD and SCvH chemical model [56] predictions respectively, also taken from [53].

Figure 3 shows the energy, entropy and pressure of the very same system as Fig. 2. Our energy is slightly higher and entropy is slightly smaller than the estimates of Ref. [53]. The pressure is computed using the viral theorem as (2K + $V)/(3L^3)$  [55], where K and V are the total kinetic and potential energies of the system. Our estimated pressure is smaller than the CEIMC value, which is close to ab initio MD calculation with local density approximation [53]. This prediction is further away from the Saumon-Chabrier-van Horn (SCvH) equations of state based on a chemical model as a mixture of hydrogen molecules, hydrogen atoms, protons, and electrons [56]. Predicting an even denser equation of state than the chemical models is in line with previous quantum Monte Carlo calculations [53, 57]. In this respect, our observation of even larger deviations from the SCvH model will reinforce the speculated implications of such findings on the Jupiter model [53, 57], such as larger core mass and lower atmospheric metallicity.

The fact that we have reached higher internal energy (K+V) but lower pressure ( $\propto 2K+V$ ) indicates our calculation obtains lower kinetic energy and higher potential energy than the CEIMC results of Ref. [53]. It is known that accuracy in the internal energy is often greater than the pressure, as the latter requires high accuracy in the kinetic and the potential energies whose errors tend to cancel out in the internal energy [58]. Likewise, we are more confident about our calculated internal energy than the pressure because the viral estimator for the pressure omits Pulay-like corrections due to incomplete optimizations [59]. We have released our codes and trained models [60]. By confirming and further reducing the variational free energy one can verify our findings reported here.

Unlike many previous studies on dense hydrogen [16, 17, 53, 57, 61], our calculation starts from a rather uninformative point with minimal physical constraints. In this regard, it is rather satisfying that the present calculation has yielded compatible equations of state for such an intensively studied system. In the future, one can also put prior knowledge such as the empirical and machine-learned potential [62] into the flow model Eq. (3). One can use them either to pretrain the flow model or replace the uniform base distribution. In the

latter case, the flow transformation corrects the base model and our variational objective function will be the free energy difference with the base model.

The calculation of Fig. 2 runs on 64 Nvidia V100 GPUs for about 60 hours. It will just be a matter of computational resources to produce the full equations of state of dense hydrogen in the atomic phase. For higher temperatures, one can take into account the thermal effect of electrons using the neural canonical transformation approach [37, 38]. At lower temperatures, intriguing physics such as quantum liquid and superconducting order may come into play. To take into account nuclear quantum effects in this case, we envision one can either generalize the proton probabilistic model to the path-integral representation [63] or adopt the neural canonical transformation approach [37, 38] for protons. In either way, we anticipate the computational cost brought by the zero-point motion of protons does not increase significantly, in contrast to conventional approaches like path-integral MD.

In this work, we have directly computed the Jacobian of the flow transformation in Eq. (3). To scale up to even larger system sizes, one may employ more efficient permutation equivariant flow models [35, 64–66]. Moreover, one may also consider more scalable optimization schemes [67] for a larger number of variational parameters. In the meantime, it may be useful to explore optimization schemes beyond the score function gradient estimator [68] for the flow model. For example, one can use the pathwise gradient estimator to exploit informations about the nuclear force [69, 70]. It is unclear whether this alternative choice will make training of the flow model more efficient. Last but not least, in conjunction with an alternative optimization approach, one could also explore the possibility of direct sampling of proton configurations with the normalizing flow.

It is believed there is a first-order atomic-to-molecular transition in the phase diagram of hydrogen [1]. Near the phase transition, there are significant difficulties related to slow equilibrium time or even lack of ergodicity in the Monte Carlo sampling of multimodal probability distributions [24]. This difficulty does not magically disappear in the variational free energy approach as they will show up as metastable states in the optimization landscape. Fortunately, the variational nature of our approach provides a clear guidance to judge and improve the qualities of various calculations, as one can always choose to believe the solution with the lowest free energy. We regard this as the most appealing feature of the present approach over the previous ones based on nested Monte Carlo sampling [16, 17].

Deep variational free energy optimization presented in this paper is a general computational framework. Both the nuclear probability distribution and the electronic wavefunction are open to further extensions. Thus, the framework holds the promise to be applied to study finite-temperature quantum matters beyond dense hydrogen.

Acknowledgments – We thank Xinyu Li, Qi Yang, and Xing-Yu Zhang for their support of computational resources. We thank Xinguo Ren and Quansheng Wu for useful discussions. This project is supported by the Strategic Priority Research Program of the Chinese Academy of Sciences un-

der Grant No. XDB30000000 and National Natural Science Foundation of China under Grant No. T2121001. This work

is also supported in part by Huawei CSTT Project "Learning Neural Physics Engines".

- Jeffrey M. McMahon, Miguel A. Morales, Carlo Pierleoni, and David M. Ceperley, "The properties of hydrogen and helium under extreme conditions," Reviews of Modern Physics 84, 1607 (2012).
- [2] E. Wigner and H. B. Huntington, "On the possibility of a metallic modification of hydrogen," The Journal of Chemical Physics 3, 764–770 (1935).
- [3] N. W. Ashcroft, "Metallic hydrogen: A high-temperature superconductor?" Physical Review Letters 21, 1748 (1968).
- [4] Ravit Helled, Guglielmo Mazzola, and Ronald Redmer, "Understanding dense hydrogen at planetary conditions," (2020), arXiv:2006.12219.
- [5] Setsuo Ichimaru, "Nuclear fusion in dense plasmas," Reviews of Modern Physics 65, 255 (1993).
- [6] Roberto Car and Michele Parrinello, "Unified Approach for Molecular Dynamics and Density-Functional Theory R." Phys. Rev. Lett 55, 2471 (1985).
- [7] Sam Azadi and W. M.C. Foulkes, "Fate of density functional theory in the study of high-pressure solid hydrogen," Physical Review B 88, 014115 (2013).
- [8] Thomas B Blank, Steven D Brown, August W Calhoun, and Douglas J Doren, "Neural network models of potential energy surfaces," The Journal of chemical physics 103, 4129–4137 (1995).
- [9] Weile Jia, Han Wang, Mohan Chen, Denghui Lu, Lin Lin, Roberto Car, Weinan E, and Linfeng Zhang, "Pushing the limit of molecular dynamics with ab initio accuracy to 100 million atoms with machine learning," in SC20: International conference for high performance computing, networking, storage and analysis (IEEE, 2020) pp. 1–14.
- [10] Bingqing Cheng, Guglielmo Mazzola, Chris J. Pickard, and Michele Ceriotti, "Evidence for supercritical behaviour of high-pressure liquid hydrogen," Nature 585, 217–220 (2020), arXiv:1906.03341.
- [11] Valentin V. Karasiev, Joshua Hinz, S. X. Hu, and S. B. Trickey, "On the liquid–liquid phase transition of dense hydrogen," Nature 600, E12–E14 (2021).
- [12] Hongxiang Zong, Heather Wiebe, and Graeme J. Ackland, "Understanding high pressure molecular hydrogen with a hierarchical machine-learned potential," Nature Communications 11, 5014 (2020).
- [13] Andrea Tirelli, Giacomo Tenti, Kousuke Nakano, and Sandro Sorella, "High-pressure hydrogen by machine learning and quantum Monte Carlo," 041105, L041105 (2022).
- [14] Hongwei Niu, Yubo Yang, Scott Jensen, Markus Holzmann, Carlo Pierleoni, and David M. Ceperley, "Stable solid molecular hydrogen above 900K from a machine-learned potential trained with diffusion Quantum Monte Carlo," (2022), arXiv:2209.00658.
- [15] W. M.C. Foulkes, L. Mitas, R. J. Needs, and G. Rajagopal, "Quantum Monte Carlo simulations of solids," Reviews of Modern Physics 73, 33–83 (2001).
- [16] Carlo Pierleoni, David M. Ceperley, and Markus Holzmann, "Coupled electron-ion monte carlo calculations of dense metallic hydrogen," Physical Review Letters 93, 146402 (2004).
- [17] Claudio Attaccalite and Sandro Sorella, "Stable liquid hydrogen at high pressure by a novel Ab Initio molecular-dynamics

- calculation," Physical Review Letters 100, 114501 (2008).
- [18] Rémi Bardenet, Arnaud Doucet, and Chris Holmes, "On Markov chain Monte Carlo methods for tall data," Journal of Machine Learning Research 18, 1–43 (2017), arXiv:1505.02827.
- [19] A. D. Kennedy and J. Kuti, "Noise without Noise: A New Monte Carlo Method," Physical Review Letters 54, 2473 (1985).
- [20] D. M. Ceperley and M. Dewing, "The penalty method for random walks with uncertain energies," Journal of Chemical Physics 110, 9812 (1999).
- [21] Florian R. Krajewski and Michele Parrinello, "Linear scaling electronic structure calculations and accurate statistical mechanics sampling with noisy forces," Physical Review B 73, 041105 (2006).
- [22] Max Welling and Yee Whye Teh, "Bayesian learning via stochastic gradient langevin dynamics," Proceedings of the 28th International Conference on Machine Learning, ICML 2011, 681–688 (2011).
- [23] Ye Luo, Andrea Zen, and Sandro Sorella, "Ab initio molecular dynamics with noisy forces: Validating the quantum monte carlo approach with benchmark calculations of molecular vibrational properties," The Journal of chemical physics 141, 194112 (2014).
- [24] Guglielmo Mazzola and Sandro Sorella, "Accelerating ab initio Molecular Dynamics and Probing the Weak Dispersive Forces in Dense Liquid Hydrogen," Physical Review Letters 118, 015703 (2017), arXiv:1605.08423.
- [25] M. Holzmann, D. M. Ceperley, C. Pierleoni, and K. Esler, "Backflow correlations for the electron gas and metallic hydrogen," Physical Review E 68, 046707 (2003).
- [26] Carlo Pierleoni, Kris T. Delaney, Miguel A. Morales, David M. Ceperley, and Markus Holzmann, "Trial wave functions for high-pressure metallic hydrogen," Computer Physics Communications 179, 89–97 (2008), arXiv:0712.0161.
- [27] Albrecht Huber, "Variational principles in quantum statistical mechanics," in *Mathematical Methods in Solid State and Su*perfluid Theory (Springer, 1968) pp. 364–392.
- [28] Note that Ref. [71] opted to integrate the Bloch equation for Gaussian density matrix instead of optimizing the variational free energy Eq. (1).
- [29] Lei Wang, "Generative models for physicists," (2018).
- [30] Shuo-Hui Li and Lei Wang, "Neural Network Renormalization Group," Physical Review Letters 121, 260601 (2018), arXiv:1802.02840.
- [31] Dian Wu, Lei Wang, and Pan Zhang, "Solving Statistical Mechanics using Variational Autoregressive Networks," Physical Review Letters 122, 080602 (2019), arXiv:1809.10606.
- [32] Linfeng Zhang, Weinan E, and Lei Wang, "Monge-Ampère Flow for Generative Modeling," (2018), arXiv:1809.10188.
- [33] M. S. Albergo, G. Kanwar, and P. E. Shanahan, "Flow-based generative models for Markov chain Monte Carlo in lattice field theory," Physical Review D 100, 34515 (2019), arXiv:1904.12072.
- [34] Gurtej Kanwar, Michael S Albergo, Denis Boyda, Kyle Cranmer, Daniel C Hackett, Sébastien Racanière, Danilo Jimenez Rezende, and Phiala E. Shanahan, "Equivariant flow-based

- sampling for lattice gauge theory," Physical Review Letters **125**, 121601 (2020), arXiv:2003.06413.
- [35] Peter Wirnsberger, George Papamakarios, Borja Ibarz, Sébastien Racanière, Andrew J. Ballard, Alexander Pritzel, and Charles Blundell, "Normalizing flows for atomic solids," (2021), arXiv:2111.08696.
- [36] Rasool Ahmad and Wei Cai, "Free energy calculation of crystalline solids using normalizing flow," Modelling Simul. Mater. Sci. Eng 30, 065007 (2021), arXiv:2111.01292.
- [37] Hao Xie, Linfeng Zhang, and Lei Wang, "Ab-initio Study of Interacting Fermions at Finite Temperature with Neural Canonical Transformation," Journal of Machine Learning 1, 38–59 (2022), arXiv:2105.08644.
- [38] Hao Xie, Linfeng Zhang, and Lei Wang, "m\* of Two-Dimensional Electron Gas: a Neural Canonical Transformation Study," (2022), arXiv:2201.03156.
- [39] Matt Hoffman, David M. Blei, Chong Wang, and John Paisley, "Stochastic Variational Inference," Journal of Machine Learning Research (2013), citeulike-article-id:10852147, arXiv:1206.7051.
- [40] See the Supplemental Material for (a) proton kinetic energy contributions to the thermodynamic quantities; (b) model architectures; (c) twist-averaged boundary conditions and (d) optimization details.
- [41] George Papamakarios, Eric Nalisnick, Danilo Jimenez Rezende, Shakir Mohamed, and Balaji Lakshminarayanan, "Normalizing flows for probabilistic modeling and inference," Journal of Machine Learning Research 22, 1–64 (2021), arXiv:1912.02762.
- [42] David Pfau, James S. Spencer, Alexander G.D.G. Matthews, and W. M.C. Foulkes, "Ab initio solution of the many-electron Schrödinger equation with deep neural networks," Physical Review Research 2, 033429 (2020), arXiv:1909.02487.
- [43] Jonas Köhler, Leon Klein, and Frank Noé, "Equivariant Flows: sampling configurations for multi-body systems with symmetric energies," (2019), arXiv:1910.00753.
- [44] Atilim Gunes Baydin, Barak A. Pearlmutter, Alexey Andreyevich Radul, and Jeffrey Mark Siskind, "Automatic differentiation in machine learning: a survey," Journal of Machine Learning 18, 1–43 (2015), arXiv:1502.05767.
- [45] Gabriel Pescia, Jiequn Han, Alessandro Lovato, Jianfeng Lu, and Giuseppe Carleo, "Neural-network quantum states for periodic systems in continuous space," Phys. Rev. Research 4, 023138 (2022).
- [46] Max Wilson, Saverio Moroni, Markus Holzmann, Nicholas Gao, Filip Wudarski, Tejs Vegge, and Arghya Bhowmik, "Wave function Ansatz (but Periodic) Networks and the Homogeneous Electron Gas," (2022), arXiv:2202.04622.
- [47] G. Cassella, H. Sutterud, S. Azadi, N. D. Drummond, D. Pfau, J. S. Spencer, and W. M. C. Foulkes, "Discovering Quantum Phase Transitions with Fermionic Neural Networks," (2022), arXiv:2202.05183.
- [48] Xiang Li, Zhe Li, and Ji Chen, "Ab initio calculation of real solids via neural network ansatz," (2022), arXiv:2203.15472.
- [49] Federico Becca and Sandro Sorella, Quantum Monte Carlo Approaches for Correlated Systems (Cambridge University Press, 2017) pp. 1–274.
- [50] Nicholas Gao and Stephan Günnemann, "Ab-Initio Potential Energy Surfaces by Pairing GNNs with Neural Wave Functions," (2021), arXiv:2110.05064.
- [51] Michael Scherbela, Rafael Reisenhofer, Leon Gerard, Philipp Marquetand, and Philipp Grohs, "Solving the electronic Schrödinger equation for multiple nuclear geometries with weight-sharing deep neural networks," (2021),

- arXiv:2105.08351.
- [52] C. Lin, F. H. Zong, and D. M. Ceperley, "Twist-averaged boundary conditions in continuum quantum Monte Carlo algorithms," Physical Review E 64, 016702 (2001).
- [53] Miguel A. Morales, Carlo Pierleoni, and D. M. Ceperley, "Equation of state of metallic hydrogen from coupled electronion Monte Carlo simulations," Physical Review E 81, 021202 (2010), arXiv:0906.1594.
- [54] Y. Miguel, T. Guillot, and L. Fayon, "Jupiter internal structure: The effect of different equations of state," Astronomy and Astrophysics 596, A114 (2016), arXiv:1609.05460.
- [55] Lev Davidovich Landau and Evgenii Mikhailovich Lifshitz, Statistical Physics: Volume 5 (Elsevier, 2013).
- [56] Didier Saumon, Gilles Chabrier, and Hugh M van Horn, "An equation of state for low-mass stars and giant planets," The astrophysical journal supplement series 99, 713 (1995).
- [57] Guglielmo Mazzola, Ravit Helled, and Sandro Sorella, "Phase Diagram of Hydrogen and a Hydrogen-Helium Mixture at Planetary Conditions by Quantum Monte Carlo Simulations," Physical Review Letters 120, 025701 (2018), arXiv:1709.08648.
- [58] B. Militzer and D. M. Ceperley, "Path integral Monte Carlo simulation of the low-density hydrogen plasma," Physical Review E 63, 066404 (2001).
- [59] Guglielmo Mazzola, Seiji Yunoki, and Sandro Sorella, "Unexpectedly high pressure for molecular dissociation in liquid hydrogen by electronic simulation," Nature communications 5, 3487 (2014).
- [60] See https://github.com/fermiflow/hydrogen for code written in Jax [72].
- [61] Carlo Pierleoni, Miguel A. Morales, Giovanni Rillo, Markus Holzmann, and David M. Ceperley, "Liquid-liquid phase transition in hydrogen by coupled electron-ion Monte Carlo simulations," Proceedings of the National Academy of Sciences of the United States of America 113, 4953–4957 (2016).
- [62] Linfeng Zhang, Jiequn Han, Han Wang, Roberto Car, and Weinan E, "Deep Potential Molecular Dynamics: A Scalable Model with the Accuracy of Quantum Mechanics," Physical Review Letters 120, 143001 (2018), arXiv:1707.09571.
- [63] Richard P Feynman, Albert R Hibbs, and Daniel F Styer, Quantum mechanics and path integrals (Courier Corporation, 2010).
- [64] Yang Li, Christopher M Bender, Haidong Yi, Siyuan Shan, and Junier B. Oliva, "Exchangeable neural ODE for set modeling," (2020), arXiv:2008.02676.
- [65] Marin Biloš and Stephan Günnemann, "Equivariant Normalizing Flows for Point Processes and Sets," (2020), arXiv:2010.03242.
- [66] Peter Wirnsberger, Andrew J. Ballard, George Papamakarios, Stuart Abercrombie, Sébastien Racanière, Alexander Pritzel, Danilo Jimenez Rezende, and Charles Blundell, "Targeted free energy estimation via learned mappings," Journal of Chemical Physics 153, 144112 (2020), arXiv:2002.04913.
- [67] James Martens and Roger Grosse, "Optimizing Neural Networks with Kronecker-factored Approximate Curvature," (2015), arXiv:1503.05671.
- [68] Shakir Mohamed, Mihaela Rosca, Michael Figurnov, and Andriy Mnih, "Monte Carlo Gradient Estimation in Machine Learning," Journal of Machine Learning Research **21**, 1–62 (2020), arXiv:1906.10652.
- [69] Sandro Sorella and Luca Capriotti, "Algorithmic differentiation and the calculation of forces by quantum Monte Carlo," Journal of Chemical Physics 133, 234111 (2010), arXiv:1010.5560.
- [70] Yubing Qian, Weizhong Fu, Weiluo Ren, and Ji Chen, "Interatomic force from neural network based variational quantum Monte Carlo," (2022), arXiv:2207.07810.

- [71] Burkhard Militzer and E L Pollock, "Variational density matrix method for warm, condensed matter: Application to dense hydrogen," Physical Review E **61**, 3470 (2000).
- [72] James Bradbury, Roy Frostig, Peter Hawkins, Matthew James Johnson, Chris Leary, Dougal Maclaurin, George Necula, Adam Paszke, Jake VanderPlas, Skye Wanderman-Milne, and Qiao Zhang, "JAX: composable transformations of Python+NumPy programs," (2018).

#### SUPPLEMENTAL MATERIAL

# Appendix A: Proton kinetic energy contributions to the thermodynamic quantities

In the Born-Oppenheimer approximation, the proton kinetic energy term is omitted in the Hamiltonian of hydrogen system. As a result, the variational density matrix is diagonal with respect to the proton coordinates S, and the variational free energy defined in Eq. (1) of the main text satisfies  $F \ge -k_B T \ln z$ , where  $z = \int dS e^{-E(S)/k_B T}$  is the partition function, and E(S) is the electronic ground-state energy of the Hamiltonian at given proton configuration S.

Once the variational free energy minimization is performed, we have to account for extra contributions of the proton kinetic energy term by considering the *full* partition function of the system:

$$Z = \frac{1}{N!h^{3N}} \int d\mathbf{P} \int d\mathbf{S} \exp\left[-\frac{1}{k_B T} \left(\frac{\mathbf{P}^2}{2m_p} + E(\mathbf{S})\right)\right]$$
$$= \frac{z}{N!A^{3N}}, \tag{A1}$$

where P is the proton momenta and  $\lambda = h/\sqrt{2\pi m_{\rm p}k_BT}$  is the thermal de Broglie wavelength of protons. h is the Planck constant and  $m_{\rm p}$  is the proton mass. The additional prefactor  $1/N!\lambda^{3N}$  in Eq. (A1) contributes to various thermodynamic quantities. Specifically, it gives an offset  $k_BT \ln(N!\lambda^{3N})$  to the free energy,  $\frac{3}{2}Nk_BT$  to the internal energy,  $\frac{Nk_BT/Ry}{(L/a_0)^3}\frac{Ry}{a_0^3} = \frac{3k_BT/Ry}{4\pi r_s^3}14710.5$ GPa to the pressure, and  $\left[\frac{3}{2}N - \ln(N!\lambda^{3N})\right]k_B$  to the entropy. All of these contributions have been taken into account in the data plots of the main text.

# Appendix B: Model architectures

In this section, we describe in detail the two neural networks that are used to construct the variational density matrix of dense hydrogen. Learnable parameters or layers are indicated in blue.

## 1. FermiNet layer

We define a generic FermiNet layer [42], shown in Algorithm 1, as a building block for the modeling of both proton Boltzmann distribution and electron wavefunction. This network maps a set of coordinates  $x_1, \ldots, x_D$  (of electrons or protons) to the same number of output features  $f_1, \ldots, f_D$  in a translation- and permutation-equivariant way. To handle an array of concatenated coordinates of protons and electrons of both spins, we introduce a split operation  $\operatorname{split}(x_{1:D}, \operatorname{idx}) := (x_{1:\operatorname{idx}(1)}, x_{\operatorname{idx}(1)+1:\operatorname{idx}(2)}, \ldots, x_{\operatorname{idx}(K)+1:D})$ , where  $\operatorname{idx}$  is an integer sequence of length K specifying the cutting point of the array. This operation can be straightforwardly generalized to higher-dimensional arrays for any given axis.  $\operatorname{FC}_n$  denotes a

fully connected layer with n output features. In our calculations, the network depth is set to be d=4 for the proton distribution and d=3 for the electron wavefunction, and the one- and two-particle feature size are  $n_1=32$  and  $n_2=16$ , respectively. The output feature size is equal to  $n_1=32$ , which we also refer to as M in the algorithm to be consistent with the main text. The number of frequencies used to construct the periodic input two-particle features is  $N_f=5$ .

## **Algorithm 1** A FermiNet layer for particles in a periodic box.

**Input:** Coordinates x, partition indices idx, and box length L. **Output:** A list of equivariant features.

```
1: h_1 = zeros\_like(x)
                                                                                           ▶ single-particle features
  2: \ \boldsymbol{x}_{ij} = \boldsymbol{x}_i - \boldsymbol{x}_j
3: h_2 = \left[ \left| \sin \left( \frac{\pi x_{ij}}{L} \right) \right| \right]
4: for m = 1, \dots, N_f do
               h_2 += \left[\cos\left(\frac{2\pi m x_{ij}}{L}\right), \sin\left(\frac{2\pi m x_{ij}}{L}\right)\right]
                                                                                               ▶ two-particle features
  7: for \ell = 1, \dots, d do
                g = [h_1,
                        mean(h, axis=0) for h in split(h_1, idx, axis=0),
                        mean(h, axis=0) for h in split(h_2, idx, axis=0)]
 9:
                if \ell = 1 then
                       \begin{aligned} & \boldsymbol{h}_1 = \tanh(\operatorname{FC}_{n_1}^{\ell}(\boldsymbol{g})) \\ & \boldsymbol{h}_2 = \tanh(\operatorname{FC}_{n_2}^{\ell}(\boldsymbol{h}_2)) \end{aligned}
10:
                                                                                                                          \triangleright \mathbb{R}^{D \times D \times n_2}
11:
12:
                       \begin{aligned} & \boldsymbol{h}_1 = \tanh(\operatorname{FC}_{n_1}^{\ell}(\boldsymbol{g})) + \boldsymbol{h}_1 \\ & \boldsymbol{h}_2 = \tanh(\operatorname{FC}_{n_2}^{\ell}(\boldsymbol{h}_2)) + \boldsymbol{h}_2 \end{aligned}
13:
14:
15:
16: end for
17: g = [h_1,
               mean(h, axis=0) for h in split(h_1, idx, axis=0),
                mean(h, axis=0) for h in split(h_2, idx, axis=0)]
                                                                                                                               \triangleright \mathbb{R}^{D \times M}
18: f = \tanh(\mathbf{FC}_M(g)) + h_1
19: return split(f, idx, axis=0)
```

#### 2. Probabilistic model for protons

The probabilistic model for proton Boltzmann distribution is a normalizing flow with a uniform base distribution, as shown in Algorithm 2. Since it only involves N proton coordinates  $S = \{s_1, \ldots, s_N\}$ , no splitting is needed, and the partition index list idx is empty.

**Algorithm 2** Normalizing flow for proton Boltzmann distribution.

```
Input: Proton coordinates S and box length L.

Output: Log-probability \ln p(S)

1: f = \text{FermiNet}(S, [], L)

2: \zeta = S + \text{FC}_3(f)

3: return \ln \left| \det \left( \frac{\partial \zeta}{\partial S} \right) \right| - \ln(L^{3N})
```

## 3. Electron wavefunction ansatz

The electron ground-state wavefunction depends on both the proton coordinates S and the electron coordinates R =

 $\{r_1^\uparrow,\ldots,r_{N/2}^\uparrow,r_1^\downarrow,\ldots,r_{N/2}^\downarrow\}$  of both spins. We thus set the partition index list to be [N,N+N/2] to separate the three coordinate sets, and feed the output features  $f^S,f^\uparrow,f^\downarrow$  of the FermiNet layer to a geminal network shown in Algorithm 3. See also the main text for detailed discussions about the network design. The resulting wavefunction is invariant to the permutation of protons, and antisymmetric to the permutation of electrons with the same spin.

## Algorithm 3 Geminal network for the electron wavefunction.

**Input:** Proton coordinates S, electron coordinates  $R = [r^{\uparrow}, r^{\downarrow}]$ , and box length L.

**Output:** Log-wavefunction  $\ln \psi_S(\mathbf{R})$ .

### Appendix C: Twist-averaged boundary conditions

We use twist-averaged boundary conditions for the electronic calculations [52]. In practice, We generate a random twist angle q for each proton configuration, and replace the momenta k by k+q in the plane-wave envelope of the geminal wavefunction, as shown in the 6th line of Alg. 3. Note that when wrapping around the periodic box, the spin-up and spin-down electrons will pick up opposite phases [57], which reflects the time-reversal symmetry of the system.

We also introduce explicit dependence on the twist q in the wavefunction ansatz to enhance its expressive power. (Not shown in Alg. 1 and Alg. 3 above for simplicity.) Firstly, we make the single-particle features  $h_1$  in the FermiNet layer depend on the twist. Secondly,  $\lambda_k$  are not standalone parameters but computed by feeding the twist q into a multilayer perceptron with softplus activation.

## **Appendix D: Optimization details**

As shown in the main text, the variational free energy is expressed as a two-fold expectation over the proton and electron coordinates S and R as follows:

$$F = \mathbb{E}_{S \sim p(S)} \left[ k_B T \ln p(S) + \mathbb{E}_{R \sim |\psi_S(R)|^2} \left[ E_S^{\text{loc}}(R) \right] \right], \quad (D1)$$

where  $E_S^{\rm loc}({\pmb R}) \equiv \frac{H\psi_S({\pmb R})}{\psi_S({\pmb R})}$  is the local energy. Denoting  $\phi$  and  $\theta$  as the parameters in the proton Boltzmann distribution  $p({\pmb S})$  and electron wavefunction  $\psi_S({\pmb R})$ , respectively, the corresponding gradients can be written as

$$\nabla_{\phi} F = \underset{S \sim p(S)}{\mathbb{E}} \left[ \nabla_{\phi} \ln p(S) \left( k_B T \ln p(S) + \underset{R \sim |\psi_S(R)|^2}{\mathbb{E}} \left[ E_S^{\text{loc}}(R) \right] \right) \right], \tag{D2a}$$

$$\nabla_{\theta} F = 2\Re \underset{S \sim p(S)}{\mathbb{E}} \left[ \underset{\boldsymbol{R} \sim |\psi_{S}(\boldsymbol{R})|^{2}}{\mathbb{E}} \left[ \nabla_{\theta} \ln \psi_{S}^{*}(\boldsymbol{R}) \cdot E_{S}^{\text{loc}}(\boldsymbol{R}) \right] \right.$$

$$\left. - \underset{\boldsymbol{R} \sim |\psi_{S}(\boldsymbol{R})|^{2}}{\mathbb{E}} \left[ \nabla_{\theta} \ln \psi_{S}^{*}(\boldsymbol{R}) \right] \underset{\boldsymbol{R} \sim |\psi_{S}(\boldsymbol{R})|^{2}}{\mathbb{E}} \left[ E_{S}^{\text{loc}}(\boldsymbol{R}) \right] \right]. \tag{D2b}$$

Note that different from Ref. [38], the ground-state wavefunction ansatz  $\psi_S(R)$  in the present work is not necessarily normalized. This results in the extra second term in the gradient estimator Eq. (D2b), which would be vanishing for normalized wavefunctions. To estimate this term accurately in practice, we sample W independent proton configurations from p(S), then given each of them we sample a *minibatch* of electron configurations of size B/W from  $|\psi_S(R)|^2$ . In the calculation, we set the batch size W = 1024 for protons and B = 8192 for electrons, respectively.

We jointly optimize the proton coordinate distribution p(S) and the electron wavefunction  $\psi_S(R)$  using the second-order stochastic reconfiguration method for variational density matrices developed in [38]. The update rules for the variational parameters reads

$$\Delta \phi = -(I + \eta \mathbb{1})^{-1} \nabla_{\phi} F, \tag{D3a}$$

$$\Delta \theta = -(\mathcal{J} + \eta \mathbb{1})^{-1} \nabla_{\theta} F, \tag{D3b}$$

where

$$I_{ij} = \underset{S \sim p(S)}{\mathbb{E}} \left[ \frac{\partial \ln p(S)}{\partial \phi_i} \frac{\partial \ln p(S)}{\partial \phi_j} \right]$$
(D4)

is the classical Fisher information matrix, and

$$\mathcal{J}_{ij} = \mathfrak{R} \int d\mathbf{S} p(\mathbf{S}) \left\langle \mathbf{S}, \frac{\partial \psi_{S}}{\partial \theta_{i}} \middle| \mathbf{S}, \frac{\partial \psi_{S}}{\partial \theta_{j}} \right\rangle - \mathfrak{R} \iint d\mathbf{S} d\mathbf{S}' \frac{2p(\mathbf{S})p(\mathbf{S}')}{p(\mathbf{S}) + p(\mathbf{S}')} \left\langle \mathbf{S}', \frac{\partial \psi_{S'}}{\partial \theta_{i}} \middle| \mathbf{S}, \psi_{S} \right\rangle \left\langle \mathbf{S}, \psi_{S} \middle| \mathbf{S}', \frac{\partial \psi_{S'}}{\partial \theta_{j}} \right\rangle \\
= \mathfrak{R} \int d\mathbf{S} p(\mathbf{S}) \left( \left\langle \frac{\partial \psi_{S}}{\partial \theta_{i}} \middle| \frac{\partial \psi_{S}}{\partial \theta_{j}} \right\rangle - \left\langle \frac{\partial \psi_{S}}{\partial \theta_{i}} \middle| \psi_{S} \right\rangle \left\langle \psi_{S} \middle| \frac{\partial \psi_{S}}{\partial \theta_{j}} \right\rangle \right) \\
= \mathfrak{R} \underset{\mathbf{S} \sim p(\mathbf{S})}{\mathbb{E}} \left[ \underset{\mathbf{R} \sim [\psi_{S}(\mathbf{R})]^{2}}{\mathbb{E}} \left[ \frac{\partial \ln \psi_{S}^{*}(\mathbf{R})}{\partial \theta_{i}} \frac{\partial \ln \psi_{S}(\mathbf{R})}{\partial \theta_{j}} \middle| - \underset{\mathbf{R} \sim [\psi_{S}(\mathbf{R})]^{2}}{\mathbb{E}} \left[ \frac{\partial \ln \psi_{S}^{*}(\mathbf{R})}{\partial \theta_{i}} \middle| \underset{\mathbf{R} \sim [\psi_{S}(\mathbf{R})]^{2}}{\mathbb{E}} \left[ \frac{\partial \ln \psi_{S}(\mathbf{R})}{\partial \theta_{i}} \middle| \right] \right] \tag{D5}$$

is the average of the quantum Fisher information matrix over proton configurations. Note only the diagonal terms survive in the double integration term of Eq. (D5), which originates from the orthogonality of the eigenstates  $|S\rangle$  for different proton configurations. We have added a small shift  $\eta = 10^{-3}$  to the diagonal of the Fisher information matrices in Eq. (D3) for numerical stability. Furthermore, the norms of updates are constrained within a threshold of  $10^{-3}$  [42].

Algorithm 4 summarizes the implementation of a single optimization step described in this section.

# Algorithm 4 An optimization step

**Input:** Proton Boltzmann distribution p(S) and electron wavefunction  $\psi_S(\mathbf{R})$ .

**Output:** Parameter updates  $\Delta \phi$ ,  $\Delta \theta$ .

- $\triangleright \mathbb{R}^{W \times N \times 3}$ 1: Sample *W* proton configurations  $S \sim p(S)$  $\triangleright \mathbb{R}^{B \times N \times 3}$
- 2: Sample *B* electron configurations  $\mathbf{R} \sim |\psi_S(\mathbf{R})|^2$
- 3: Estimate the gradients Eq. (D2)
- 4: Estimate the Fisher information matrices Eqs. (D4) and (D5)
- 5: **return** Parameter updates according to Eq. (D3)